J|A|C|S
ARTICLES
Published on Web 11/08/2002

Placement and Characterization of Pairs of Luminescent Molecules in Spatially Separated Regions of Nanostructured Thin Films

Payam N. Minoofar,[†] Raquel Hernandez,[†] Shinye Chia,[†] Bruce Dunn,[†] Jeffrey I. Zink,*[,†] and Anne-Christine Franville[‡]

Contribution from the Department of Chemistry and Biochemistry, Department of Materials Science and Engineering, University of California, Los Angeles, Los Angeles, California 90095, and Laboratoire des Matériaux Inorganiques, Université Blaise Pascal and ENSCCF, 24 av. des Landais, 63174 AUBIERE Cedex, France

Received June 10, 2002

Abstract: Methods of making mesostructured sol−gel silicate thin films containing two different molecules deliberately placed in two different spatially separated regions in a one-step, one-pot preparation are developed and demonstrated. When the structure-directing agent is the surfactant cetyltrimethylammonium bromide, the structure is 2-D hexagonal with lattice spacings between 31.6 and 42.1 Å depending on the dopant molecules and their concentrations. The three general strategies that are used to place the molecules are philicity (like dissolves like), bonding, and bifunctionality. These strategies take advantage of the different chemical and physical properties of the regions of the films. These regions are the inorganic silicate framework, the hydrophobic organic interior of the micelles, and the ionic interface between them. Luminescent molecules that possess the physical and chemical properties appropriate for the desired strategies are chosen. Lanthanide and ruthenium complexes with condensable trialkoxysilane groups are incorporated into the silicate framework. 1,4-Naphthoquinone, pyrene, rhodamine 6G and coumarin 540A, and lanthanides with no condensable trialkoxysilanes occupy the hydrophobic core of micelles by virtue of their hydrophobicity. The locations of the molecules are determined by luminescence spectroscopy and by luminescence lifetime measurements. In all cases, the long-range order templated into the thin film is verified by X-ray diffraction. The simultaneous placement of two molecules in the structured film and the maintenance of long-range order require a delicate balance among film preparation methodology, design of the molecules to be incorporated in specific regions, and concentrations of all of the species.

Introduction

Incorporation of photoactive molecules in specific regions of mesostructured silicate films is attracting increasing interest. Several methods of preparing the films are being explored. One of the methods involves preparing and calcining the films, then backfilling the pores with the desired molecules.[1−8] When the molecules contain alkoxysilane groups, they can be used to derivatize the newly exposed pore surfaces. An alternative method exploits a one-step, one-pot synthesis.[9] In this approach, all components — including the photoactive molecules and the structure directing agents — are dissolved in the starting sol. The dip coating[10−13] of this sol onto a substrate produces, in a single step, doped mesostructured films. The advantages to this methodology are easier and more rapid incorporation of dopants, higher doping levels than are achievable by backfilling, and access to regions other than empty pores.

The earliest one-step, one-pot preparations of films used luminescent molecules that were designed to probe the film formation.[10−12] In these studies, a luminescent probe was used to monitor micelle formation and to correlate this process with changes in solvent composition during the rapid film formation. Probes that were preferentially incorporated in and report the properties of specific regions of the film were therefore used,

* To whom correspondence should be addressed. E-mail: zink@chem.ucla.edu.
[†] University of California, Los Angeles.
[‡] Université Blaise Pascal and ENSCCF.

(1) Clark, J. H.; Macquarrie, D. J. *Chem. Commun.* **1998**, *8*, 853.
(2) Liu, J.; Feng, X.; Fryxell, G. E.; Q., W. L.; Kim, A. Y.; Gong, M. *Adv. Mater.* **1998**, *10*, 161.
(3) Macquarrie, D. J.; Jackson, D. B. *Chem. Commun.* **1997**, *18*, 1781.
(4) Mercier, L.; Pinnavaia, T. J. *Adv. Mater.* **1997**, *9*, 500.
(5) Moller, L.; Bein, T.; Fischer, R. *Chem. Mater.* **1998**, *10*, ??.
(6) Shephard, D. S.; Zhou, W.; Maschmeyer, T.; Matters, J. M.; Roper, C. L.; Parsons, S.; Johnson, B. F. G.; Duer, M. J. *Angew. Chem., Int. Ed.* **1998**, *37*, 2719.
(7) Nguyen, T.; Wu, J.; Doan, V.; Schwartz, B.; Tolbert, S. *Science* **2000**, *288*, 652−656.
(8) Clark, T.; Ruiz, J. D.; Fan, H.; Brinker, C. J.; Swanson, B. I.; Parikh, A. N. *Chem. Mater.* **2000**, *12*, 3879−3884.
(9) Hernandez, R.; Franville, A.-C.; Minoofar, P.; Dunn, B.; Zink, J. I. *J. Am. Chem. Soc.* **2001**, *123*, 1248−1249.
(10) Lu, Y.; Gangull, R.; Drewlen, C. A.; Anderson, M. T.; Brinker, C. J.; Gong, W.; Guo, Y.; Soyez, H.; Dunn, B.; Huang, M. H.; Zink, J. I. *Nature* **1997**, *389*, 364−368.
(11) Huang, M. H.; Dunn, B. S.; Soyez, H.; Zink, J. I. *Langmuir* **1998**, *14*, 7331.
(12) Huang, M. H.; Soyez, H.; Dunn, B. S.; Zink, J. I. *Chem. Mater.* **2000**, *12*, 231−235.
(13) Huang, M. H.; Dunn, B. S.; Zink, J. I. *J. Am. Chem. Soc.* **2000**, *122*, 3739−3745.

10.1021/ja020817n CCC: $22.00

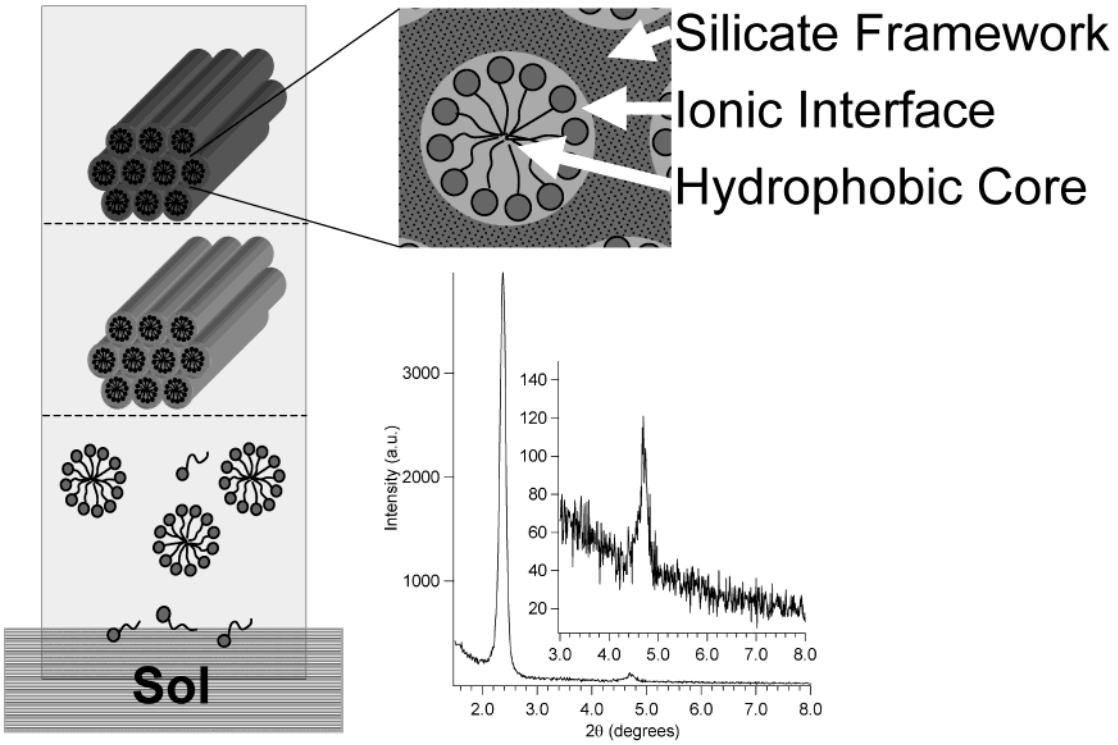

Figure 1. Pictorial representation of the film formation process. Left: processes that occur as the substrate is withdrawn from the sol. The spatially and temporally separated steps, from bottom to top, are micelle formation, network formation, and silicate condensation that locks the mesostructure into place. Top right: enlargement of the final film showing the three distinct regions. Bottom right: a typical XRD pattern from a two-dimensional, hexagonal packing of CTAB cylindrical micelles in a thin film drawn from the sol containing both R6G and C540A.

and the final films contained the luminescent molecules in the specific locations.[14,15] Efforts to modify the composition of the silicate framework itself have also been reported.[16−32] Typical studies use organically substituted alkoxysilane precursors such as $RSi(OR')_3$, where R is an alkyl or aryl group. These groups were chosen because of their hydrophobic properties, not optical function. Recently, deliberate placement of luminescent molecules in three spatially separated regions of mesostructured films templated by ionic surfactants was reported.[9] These regions were defined as the silicate matrix, the hydrophobic core of surfactant micelles, and the intervening ionic interface between surfactant headgroups and the silica framework. Designed placement of two or more molecules is also feasible but has not yet been demonstrated.

A caveat to the one-step approach is that the formation of structured films with long-range order is a delicate process that can be easily disrupted. The long-range order is especially sensitive to the presence of dopant molecules. Even the relative humidity and the concentration of alcohol vapor in the film-pulling environment can drastically affect the structure. In addition, the film quality is sensitive to the composition of the initial sol; the acidity and concentrations of reactants severely constrain the range of preparations that can be used successfully.

In this paper, we demonstrate dual placement of luminescent molecules in a one-step, one-pot dip-coating process schematically illustrated in Figure 1. We also demonstrate general strategies for placing the molecules in desired regions. The long-range ordered structure is verified for all of the films by using X-ray diffraction. In all of the cases illustrated here, we chose the two-dimensional hexagonal structure templated by cetyltrimethylammonium bromide (CTAB). We verify the incorporation of the molecules by their characteristic luminescence and verify their locations by spectroscopy and by luminescence lifetime measurements. Four categories of placement are shown. First, luminescent metal complexes in the silica framework and luminescent organic molecules in the organic region are studied. Second, luminescent metal complexes in the silica framework and luminescent metal complexes in the organic region are prepared. Third, dual placement of both a metal complex and an organic molecule in the framework and, fourth, dual

(14) Franville, A.; Dunn, B.; Zink, J. I. *J. Phys. Chem. B* **2001**, *105*, 10335−10339.
(15) Wu, J.; Abu-Omar, M. M.; Tolbert, S. *Nano Lett.* **2001**, *1*, 27−31.
(16) Asefa, T.; MacLachlan, M. J.; Coombs, N.; Ozin, G. A. *Nature* **1999**, *402*, 867−871.
(17) Babonneau, F.; Leite, L.; Fontlupt, S. *J. Mater. Chem.* **1999**, *9*, 175.
(18) Burkett, S. L.; Sims, S. D.; Mann, S. *Chem. Commun.* **1996**, 1367.
(19) Corriu, R. J. P.; Hoarau, C.; Mehdi, A.; Reye, C. *Chem. Commun.* **2000**, 71.
(20) Fowler, C. E.; Burkett, S. L.; Mann, S. *Chem. Commun.* **1997**, 1769.
(21) Inagaki, S.; Guan, S.; Fukushima, Y.; Ohsuma, T.; Terasaki, O. *J. Am. Chem. Soc.* **1999**, *121*, 9611.
(22) Lebeau, B.; Fowler, C. E.; Hall, S. R.; Mann, S. J. *J. Mater. Chem.* **1999**, *9*, 2279.
(23) Lim, M. H.; Stein, A. *Chem. Mater.* **1999**, *11*, 3285.
(24) Macquarrie, D. J. J., D. B.; Mdoe, J. E. G.; Clark, J. H. *New J. Chem.* **1999**, *23*, 539.
(25) Melde, B. J.; Holland, B. T.; Blanford, C. F.; Stein, A. *Chem. Mater.* **1999**, *11*, 3302.
(26) Ishii, C. Y.; Asefa, T.; Coombs, N.; MacLachlan, M. J.; Ozin, G. A. *Chem. Commun.* **1999**, 2539−2540.
(27) Gross, A.; Tolbert, S. *J. Phys. Chem. B* **1999**, *103*, 2374−2384.
(28) Asefa, T.; Yoshina-Ishii, C.; MacLachlan, M. J.; Ozin, G. A. *J. Mater. Chem.* **2000**, *10*, 1751−1755.
(29) Dag, O.; Yoshina-Ishii, C.; Asefa, T.; MacLachlan, M. J.; Grondey, H.; Coombs, N.; Ozin, G. A. *Adv. Funct. Mater.* **2001**, *11*, 213−217.
(30) Fan, H.; Lu, Y.; Assink, R. A.; Lopez, G. P.; Brinker, C. J. *Mater. Res. Soc. Symp. Proc.* **2001**, *628*, CC6.41.41−CC46.41.47.
(31) Kruk, M.; Asefa, T.; Tewodros, J.; Ozin, G. A. *J. Am. Chem. Soc.* **2002**, *124*, 6383−6392.
(32) Soten, I.; Ozin, G. A. Mesoscale materials synthesis and beyond. In *Supramolecular Organization and Materials Design*; Jones, W., Rao, C., Eds.; Cambridge University Press: New York, 2002; pp 34−82.

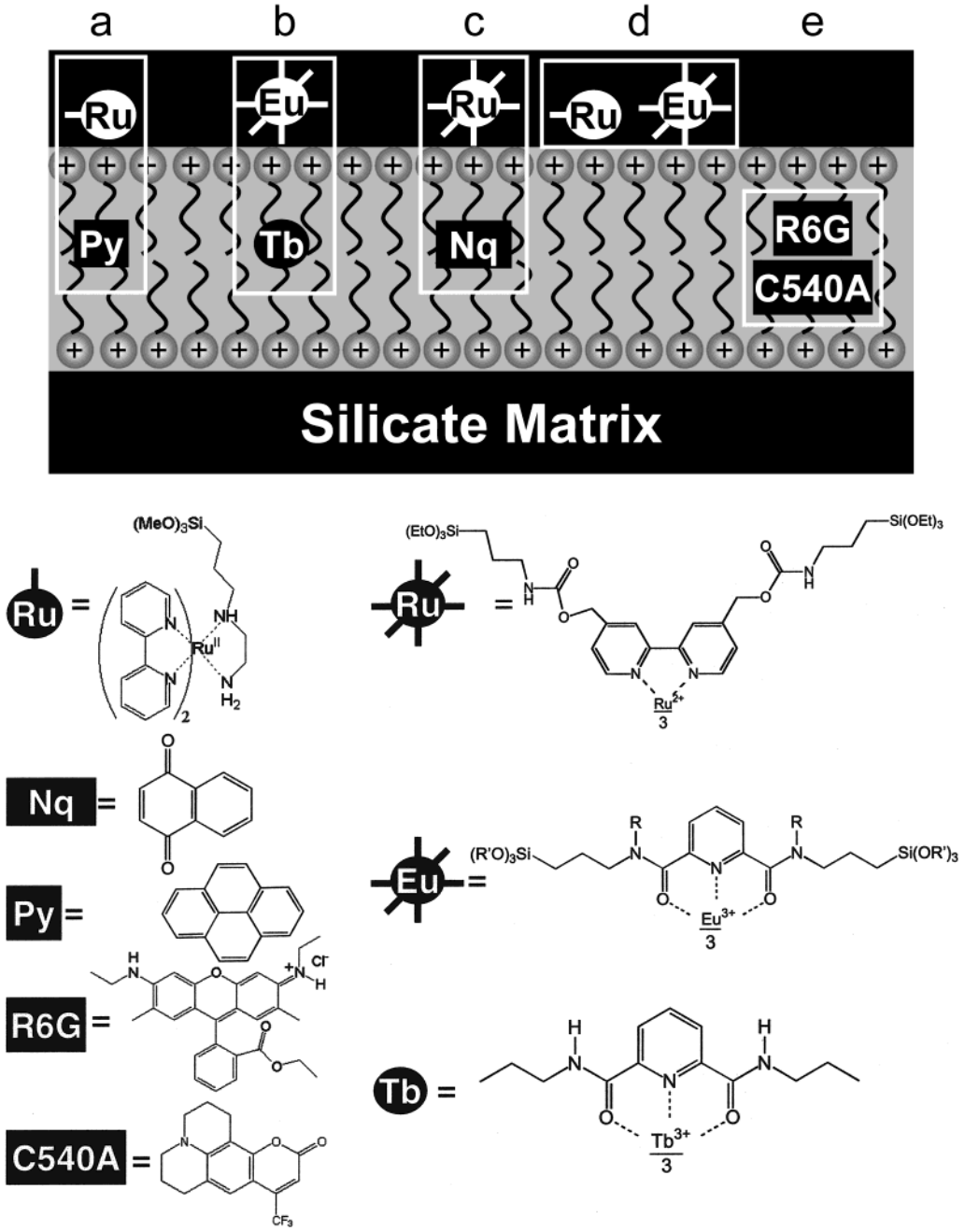

Figure 2. Schematic of the cross section along the cylinder axis of a mesostructured film. The locations of the pairs of molecules are indicated by the symbols defined below. The pairs of molecules are enclosed by white boxes and shown in the order in which they appear in the text. Appearing below the schematic is a key showing the chemical structure corresponding to each stick figure. Two different ligands are used. For SL (b), R = H and R′ = ethyl. For S4 (d), R = phenyl and R′ = methyl.

placement of two different organic molecules in the organic region are reported.

Experimental Section

Preparation of the Sol Precursor and Silicon Substrates. TEOS, ethanol, water, and HCl (1:3.8:1:5 × 10^{-5} molar ratios) are refluxed at 60 °C for 90 min to form the stock solution that is used in all of the following preparations. Films are obtained by dip coating sols onto clean silicon wafers at a withdrawal rate between 5 and 12 cm/min. The silicon wafers were cut into 1-cm wide strips and cleaned in hot "piranha" solution (H_2O_2/H_2SO_4; 1:4 by volume) for 10 min, followed by a rinse with boiling water.

Preparation of Ruthenium/Pyrene Films. First, 0.173 g of tris-(2.2′-bipyridine) ruthenium(II) chloride ($Ru(bpy)_2Cl_2$) (Aldrich), 12 mL of ethanol, 5 mL of deionized water, and 80 μL of 2-aminoethyl-2-aminopropyl trimethoxysilane (ATT) (Gelest) are placed in a plastic beaker and stirred and heated in a water bath to 60 °C until the ruthenium is completely dissolved. The color of the solution changes from purple to red-orange, indicating the formation of $Ru(bpy)_2ATT$ (Figure 2, bottom). The solvent is removed under nitrogen, and the product is redissolved in 23 mL of ethanol. In another beaker, the TEOS sol is formed by stirring 10 mL of stock solution, 1.2 mL of 0.07 N HCl, and 0.4 mL of deionized water for 15 min. The ruthenium solution is added dropwise to the TEOS sol. Next 300 μL of 1 × 10^{-3} M pyrene (Figure 2) ethanol solution is added and stirred. Amorphous films are pulled from this final solution. Next 3.5 wt % CTAB is added, the solution is stirred again, and 2-D hexagonal films are pulled.

Preparation of Europium/Terbium Film. *N*,*N*-Bis(3-triethoxysilylpropyl)-2,6-pyridine-dicarboxamide (SL, bis-silylated ligand) and *N*,*N*-bis(*n*-butyl)-2,6-pyridine-dicarboxamide (OL, organic ligand) were prepared as described previously.[33] The organic complex with terbium is obtained by refluxing a mixture of OL ligands with a terbium chloride salt ($TbCl_3 \cdot 5H_2O$) in acetonitrile, using a 1:3 Tb^{3+} to OL molar ratio. The white precipitate that is formed after 4 h of heating is recovered by filtration, washed with the reaction solvent, and finally dried under vacuum to give the complex $Tb(OL)_3Cl_3$, designated as Tb:OL. Mesostructured luminescent hybrid films co-activated with europium and terbium have been prepared, where Eu^{3+} is coordinated to bis-silylated ligands, and Tb^{3+} is introduced in the form of Tb:OL organic complexes (Eu:SL/Tb:OL films, Figure 2b, top). Complexation of Eu^{3+} ions by the SL ligand is directly performed in the sol as described below.

In a typical preparation, SL molecules are first dissolved in the stock solution (SL:TEOS = 1:19). Distilled water and HCl (0.07 N) are added to make the concentration of HCl 7.34 mM, and the mixture is then stirred for 15 min and aged at room temperature for an additional 15 min. This solution is diluted with ethanol to obtain the final composition 0.053 SL/1 TEOS/24.75 EtOH/5.64 H_2O/0.0044 HCl. After two successive 15 min periods of stirring and aging, europium chloride is introduced in the solution, and the sol is stirred at room temperature for 45 min. Addition of Tb:OL molecules and surfactant (4.0 wt % CTAB) yields the sol from which the films are pulled. The Eu^{3+}:SL:(Tb:OL) molar ratio used is 1:3:1. Amorphous films with similar compositions (excluding CTAB) were also prepared as reference samples using the same procedure as above.

Preparation of Ru/Naphthoquinone Films. 4,4′-Hydroxymethyl-2,2′-bipyridine ($bpy(CH_2OH)_2$) and $[Ru\{bpy(CH_2OH)_2\}_3](PF_6)_2$ were prepared according to the literature methods.[34,35] $[Ru\{bpy(CH_2OH)_2\}_3](PF_6)_2$ (72.2 mg, 0.0694 μmol) and a slight excess of isocyanatopropyltriethoxysilane (ICPES: ~100 μL, 0.4 mmol) were added to ~10 mL of anhydrous DMF under nitrogen followed by 20 h of reflux. The solvent was removed under vacuum at elevated temperature to yield a dark red oil. The coupling reaction was confirmed by the formation of carbamate and the disappearance of the CO stretch (ν = 2272 cm^{-1}) of the isocyanato group. IR (KBr): ν = 1718 cm^{-1} (carbamate C═O).

The stock solution (5.0 mL), water (0.20 mL), and HCl (0.07 N, 0.6 mL) were mixed and stirred for 15 min before the addition of ruthenium complex (ethanolic solution of the silanized $Ru(bpy)_3(PF_6)_2$, 11.6 mL). The ruthenium complex was coupled to ICPES at the last step to avoid possible hydrolysis and condensation of the ethoxy groups during the multistep synthesis. ICPES was coupled to the derivatized $Ru(bpy)_3^{2+}$ with two hydroxyl groups on each ligand through the formation of carbamates (Figure 2, bottom).

1,4-Naphthoquinone (NQ, Figure 2, bottom) was added with stirring to the sol. The final sol containing the ruthenium complex and NQ was used for dip-coating the silicon substrates (Figure 2c, top). Using the same batch of sol, CTAB (2.5−4.0 wt % of the final sol mixture) was then added slowly to the sol and used to make the structured film.

Preparation of Europium/Ruthenium Films. The silylated ligand bis(*N*,*N*-phenyl,3-trimethoxysilylpropyl)-2,6-pyridinedicarboxamide (S4) for europium was prepared as described previously,[33] and 1.05 g of this ligand was dissolved in 80 mL of the stock solution. Next 7.5 mL of this solution was mixed with 0.9 mL of 0.07 M HCl and 0.3 mL of water. This mixture was stirred for 15 min and allowed to age 15 min more. Next 19 mL of ethanol was added to the mixture, and stirring resumed. Next 19.5 mg of $EuCl_3 \cdot 6H_2O$ (1/3 mol equiv of S4 present in the sol) was thoroughly dissolved in the sol. In a separate beaker, the singly tethered ruthenium complex, $Ru(bpy)_2ATT$, was prepared as described above, and the final product was reconstituted in a few milliliters of ethanol. The Eu containing sol was then added to this concentrated ethanol solution, and, after brief stirring, one film was drawn onto a clean silicon substrate. Next 0.76 g of CTAB (3.5% by mass) was dissolved in the sol, and another film was drawn onto silicon (Figure 2d, top). The final ratio of metals in each sol was Si:Ru:Eu 348:4:1.

Preparation of Rhodamine 6G/Coumarin 540A Films. The stock solution (7.5 mL) was stirred with 0.9 mL of 0.07 M HCl and 0.3 mL of doubly deionized water for 15 min. After 15 additional min of aging, 19 mL of ethanol was added. Subsequently, 0.94 mg (by addition of 1 mL of a 2.0 mM ethanol solution) of rhodamine 6G (R6G) and 0.0108 g of coumarin 540A (C540A) were dissolved in the sol, and amorphous films were dip coated onto clean silicon wafers (Figure 2e, top). Next 0.76 g of CTAB (3.5% by mass) was dissolved in the sol, and mesostructured films were pulled. The ratio of R6G to C540A in the sol was 1:18. Control films containing individual dyes were prepared in the same manner.

Characterization Methods. The film structure was characterized by X-ray diffraction (XRD) patterns recorded in the 2θ range 1.50−8.00° on a Siemens D500 diffractometer using Cu $K_{\alpha 1}$ radiation (λ = 1.5418 Å). Experimental uncertainty in 2θ was ±0.05°, corresponding to an uncertainty of ±0.8 Å in the reported *d* spacings.

Fluorescence spectra from the Ru/Py and Ru/NQ films were obtained on a FL3-22 (Jobin-Yvon/ISA Spex) spectrofluorometer. Excitation and emission spectra for the Eu/Ru films and R6G/C540A films were obtained from a Spex model 1902 spectrofluorometer. Absorption spectra were obtained from a Shimadzu UV3101-PC UV−vis−NIR spectrophotometer. All spectra were obtained at room temperature.

Ru emission lifetimes in the Ru/NQ films were measured with a pulsed laser system. An optical parametric oscillator (Opotek, Inc.) pumped by the third harmonic of a Nd:YAG (Quantel Brilliant, 20 Hz, 20 mJ/pulse) was used as the excitation source (460 nm). The luminescence emission was passed through a 545 nm cutoff filter, directed into a single monochromator (SPEX 1702), and then detected by a photomultiplier tube (RCA C31034) at 620 nm for silanized $Ru(bpy)_3^{2+}$ or 605 nm for $Ru(bpy)_3^{2+}$. The signal from the PMT, the lifetime decay curve, was recorded by a digitizing oscilloscope (Tektronix RTD710) with a 50 Ω terminator. Each measurement was averaged over 1024 pulses and carried out at room temperature. Luminescence decay curves were fit with the computer program IGOR. Multiple decay curves were obtained from each sample, and the lifetimes obtained from these fits were averaged. Each calculated lifetime contained a 10% uncertainty based on the standard deviation from multiple measurements.

For the Eu/Tb films, emission spectra were recorded by exciting the samples with the 290.0 nm radiation extracted from the KDP-doubled laser beam delivered by a Nd:YAG laser working with a mixture of rhodamine dyes (Rh590 + Rh610). Direct excitation in the Eu^{3+}-$^5D_0$ or Tb^{3+}-$^5D_4$ levels was obtained by using the direct output beam of the continuum dye laser working with a mixture of Rh590−Rh610 and Rh610−Rh640 for europium and terbium, respectively. The emitted light was focused at the entrance slit of a JobinYvon HR1000 monochromator and detected with a R1104 Hamamatsu photomultiplier. Fluorescence lifetimes were measured with a Lecroy 9310A Dual 400 MHz digital oscilloscope. In the case of Eu and Tb luminescence lifetime measurements, uncertainties were smaller than ±0.04 ms. Excitation spectra were obtained with the Fluorolog FL3-22 spectrofluorometer by monitoring the most intense emission transition peaking at 616.0 or 544.3 nm in the case of europium and terbium, respectively.

Results

Ruthenium/Pyrene Films. The ruthenium/pyrene film has an XRD peak at 2θ equal to 2.60° corresponding to a *d* spacing of 34.0 Å. The ruthenium complex, in both the mesostructured

(33) Franville, A.; Zambon, D.; Mahiou, R. *Chem. Mater.* **2000**, *12*, 428−435.
(34) Kocian, O.; Mortimer, R. J.; Beer, P. D. *Tetrahedron Lett.* **1990**, *31*, 5069−5072.
(35) Collins, J. E.; Lamba, J. J. S.; Love, J. C.; McAlvin, J. E.; Ng, C.; Peters, B. P.; Wu, X.; Frasier, C. L. *Inorg. Chem.* **1999**, *38*, 8.

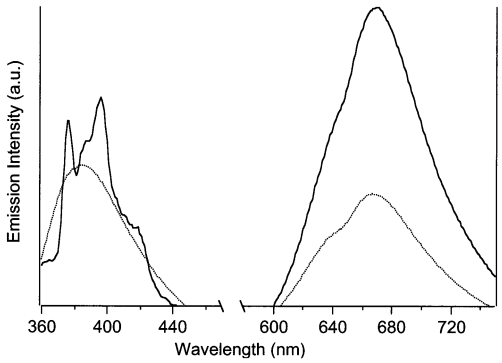

Figure 3. Emission spectra of the $Ru(bpy)_2(ATT)^{2+}$ and pyrene pair in thin films. The upper lines are the spectra from a 2-D hexagonally structured film, and the lower lines are the spectra from an amorphous film. The emission in the region of 400 nm arises from the pyrene molecules excited at 351 nm, and that in the 670 nm region arises from the ruthenium complex excited at 488 nm.

film and the amorphous film, has an emission maximum at 669 nm, as shown in Figure 3. Previously it was shown that the ruthenium peak maximum shifted from 665 to 650 nm when it was located in the organic region of a lamellar structured film.[9] Pyrene, in the mesostructured film, shows a well-resolved vibronic structure with maxima at 375 (peak I), 385 (peak III), and 394 nm in agreement with literature values (Figure 3).[36] In the amorphous film, the vibronic structure is not resolved, and a broad single peak at 386 nm is observed.

Europium/Terbium Films. The XRD pattern recorded for the CTAB-templated Eu:SL/Tb:OL hybrid thin films is typical of a 2-D hexagonal mesophase, with a *d* spacing of 42.1 Å (d_{100}).

Emission spectra obtained at room temperature under UV excitation for Eu:SL/Tb:OL amorphous and mesostructured thin films are displayed in Figure 4. These spectra exhibit quite similar features and show the luminescence of both Eu^{3+} and Tb^{3+} ions, with the characteristic $^5D_0 \rightarrow {}^7F_J$ ($J = 0-4$) and $^5D_4 \rightarrow {}^7F_J$ ($J = 3-6$) emission lines for europium and terbium, respectively. Using 290.0 nm excitation, emission from Eu^{3+} or Tb^{3+} arises from the ATE (absorption-transfer-emission) mechanism, which is well known for rare-earth organic complexes.[37] The emission intensity from terbium is much higher than that from europium, due to a more efficient sensitization of its fluorescence via the triplet state of the ligand. Direct excitation of the $^5D_0$ and $^5D_4$ excited levels of europium and terbium, respectively, enables the contribution of each ion in the emission of the samples to be isolated. The resulting spectra recorded for Eu:SL/Tb:OL mesostructured films are presented in Figure 4c and d. The shape of the Eu^{3+} emission spectrum is the same in both the mesostructured and the amorphous films. In particular, the ratios of the $^5D_0 \rightarrow {}^7F_2$ and $^5D_0 \rightarrow {}^7F_1$ transitions intensities, which are sensitive to the symmetry around the ion, remain identical. Similarly, no apparent change in the terbium emission characteristics is observed in the presence of the surfactant templating molecules.

Fluorescence decays recorded for the 616.0 nm europium emission in mesostructured and amorphous samples can be fit by a single-exponential function, with corresponding lifetime values of 1.02 and 1.05 ms, respectively. Fluorescence decays of the Tb^{3+} $^5D_4 \rightarrow {}^7F_5$ emission at 545.0 nm are also purely

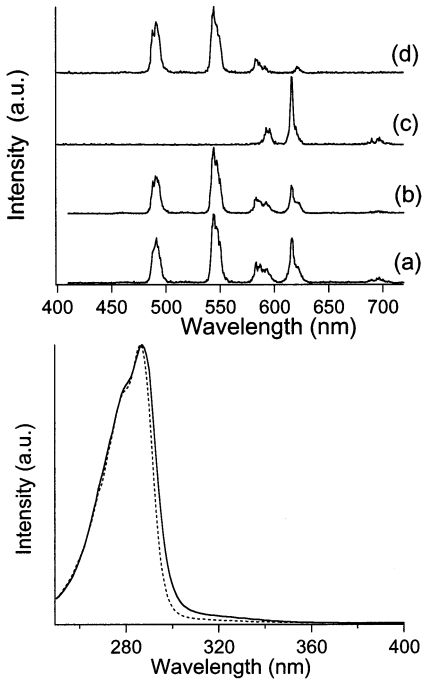

Figure 4. Emission and excitation spectra of the Eu:SL/Tb:OL pair of molecules in thin films. The spectra were obtained from amorphous (a) and mesostructured (b) films excited at 290 nm. (c) and (d) correspond respectively to the emission of only the europium complex and only the terbium complex in the mesostructured film excited at 580.5 nm (c) and 487.0 nm (d). Bottom panel: excitation spectra obtained by monitoring the Tb^{3+} emission at 545.0 nm for Eu:SL/Tb:OL mesostructured (—) and amorphous (- - -) films.

monoexponential for both types of Eu:SL/Tb:OL films. The fluorescence lifetime recorded for the Tb:OL complexes is slightly longer when the molecule is incorporated within the hexagonal mesophase (0.98 ms versus 0.89 ms in the amorphous film). The intensity ratio between the $^5D_4 \rightarrow {}^7F_5$ emission of Tb^{3+} and the $^5D_0 \rightarrow {}^7F_2$ emission of Eu^{3+} is higher in the CTAB-templated film (2.4 and 1.5 in mesostructured and amorphous films, respectively). The above two results may be related to less important nonradiative relaxation pathways in the presence of CTAB. Figure 4 (bottom) shows the excitation spectra of the Tb^{3+} fluorescence at 545.0 nm for amorphous and mesostructured hybrid films incorporating Tb:OL complexes. The onset of the broad excitation band corresponding to the $\pi \rightarrow \pi^*$ transition in OL is shifted slightly toward higher energy in the presence of CTAB molecules. Such a shift can be correlated with a modification of the Tb:OL environment in the templated films. In contrast, the shapes of the Eu^{3+} excitation spectra are unchanged for amorphous and mesostructured films.

Ruthenium/1,4-Naphthoquinone Films. The XRD patterns show a first-order diffraction pattern at $2\theta = 2.38°$, corresponding to a *d* spacing of 37.1 Å. Emission from ruthenium complexes excited at 455−470 nm and emission from NQ excited at 330 nm were collected from the front face of the films. The Ru emission maximum was at 615 nm in both the amorphous and the mesostructured films. The shoulder appearing at lower energy arises from vibronic structure. The NQ emission maximum was at 392 nm in the mesostructured films. All emission maxima have an uncertainty of ±2 nm. These spectra are shown in Figure 5. NQ emission could not be obtained from amorphous films.

(36) Kalyanasundaram, K.; Thomas, J. K. *J. Am. Chem. Soc.* **1977**, *99*, 2041−2044.
(37) Crosby, G.; Whan, R.; Alire, R. *J. Chem. Phys.* **1961**, *34*, 743.

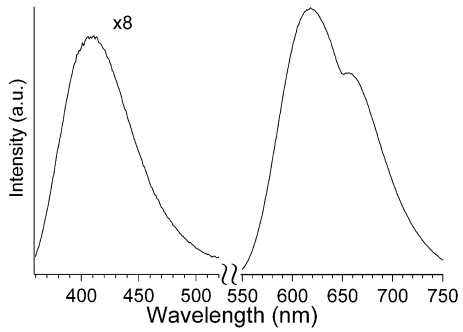

Figure 5. Luminescence spectra of the silanized $Ru(bpy)_3(PF_6)_2$ and 1,4-naphthoquinone pair of molecules in silica films. Left: emission of 1,4-naphthoquinone (excited at 330 nm) in a mesostructured film. Right: emission of silanized $Ru(bpy)_3(PF_6)_2$ (excited at 460 nm).

Table 1. Summary of Lattice Spacings, and Emission and Excitation Maxima of Mesostructured Films Containing Pairs of Molecules

			λ_{max}, emission (nm)		λ_{max}, excitation (nm)	
pair	2θ (deg)	d (Å)	amorphous	hexagonal	amorphous	hexagonal
Ru	2.60	34.0	669	669		
Py			386	375, 385, 394		
Eu	2.10	42.1	616	616		
Tb			545	545		
Ru	2.38	37.1	615	614		
Nq			none observed	392		
Eu	2.80	31.6	616	616	294	294
Ru			~670	~670	291	288
R6G	2.38	37.1	562	569	530	541
C540A			523	521	437	438

Table 2. Summary of Emission Lifetime Data for Mesostructured Films Containing Ru and NQ

sample	τ_1 (μs)	τ_2 (ns)	$\%\tau_1$[a]
Ru, no CTAB	1.47	265	34.4
Ru	1.94	310	31.4
Ru/NQ	2.09	309	33.8
Ru/2NQ	1.93	295	33.5

[a] The percentage of the long lifetime component was calculated according to the following: $\%\tau_1 = 100 \times [\alpha_1\tau_1/(\alpha_1\tau_1 + \alpha_2\tau_2)]$.

The Ru luminescence decay curves were best fit by a double-exponential function, $D(t) = \alpha_1 \exp(-t/\tau_1) + \alpha_2 \exp(-t/\tau_2)$, and the calculated lifetimes are reported in Table 2.

Europium/Ruthenium Films. Films obtained prior to addition of CTAB show no diffraction patterns in the 2θ range 1.50−8.00°. Films containing CTAB show a strong first-order diffraction peak at 2.80° (d = 31.6 Å).

Fluorescence spectra show sharp emission lines at 592, 616, and 694 nm superimposed on a broad envelope that peaks at approximately 670 nm (Figure 6). Films containing only Eu-S4 exhibit three sharp peaks at 592, 616, and 694 nm, with the 616 nm peak as the most prominent peak. The broad emission peaking at 670 nm is absent from these control films. The 670 nm emission is the same as that observed in the Ru-Py system discussed above.

R6G/C540A Films. The 2θ values for films containing laser dyes were as follows: 2.44° (d_{100} = 36.2 Å) for the film containing R6G only, 2.46° (d_{100} = 35.9 Å), and 2.38° (d_{100} = 37.1 Å) for films containing both R6G and C540A at the same concentration as the respective controls.

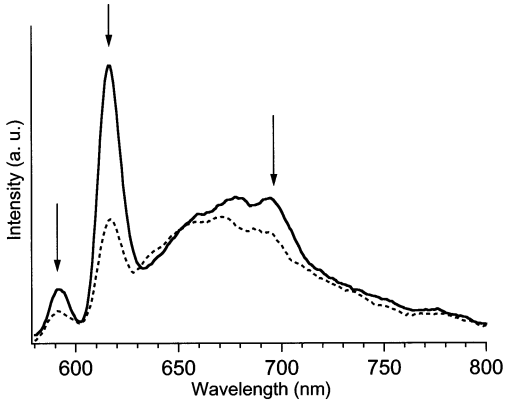

Figure 6. Luminescence spectra of the Eu-S4 and $Ru(bpy)_2ATT$ pair of molecules in amorphous (dashed line) and mesostructured (solid line) films excited at 300 nm. The arrows indicate the emission lines from the europium complex.

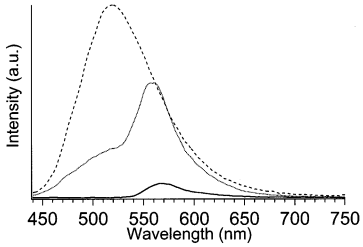

Figure 7. Luminescence spectra of R6G and C540A in mesostructured thin films. The middle trace is the spectrum from the pair of molecules, the bottom trace from only R6G, and the top trace from only C540A. All of the spectra were excited at 420 nm.

Table 1 contains a summary of the emission and excitation results obtained from films containing either R6G or C540A. There are red shifts of 11 nm in the excitation and 7 nm in the emission maxima of R6G in mesostructured films relative to the maxima in the spectra from amorphous films. The band maximum of C540A is invariant under different film structures. The fluorescence intensity of R6G is higher by a factor of 25 in mesostructured films relative to amorphous films, and that of C540A is higher by a factor of 10. Fluorescence spectra collected from films containing both laser dyes consist of the overlapping characteristic emission envelopes of the individual dyes (Figure 7).

Discussion

The primary focus of this paper, and the common thread in the experiments, is the synthesis of highly ordered, functional materials through methods that allow for a great measure of control over the final structure of the material *and* the ultimate location of the dopants that make these materials functional. Such control is essential to the implicit goal of designing the properties of mesostructured materials. The goals of this paper are to delineate the three regions of mesostructured sol−gel thin films according to their respective physical and chemical properties and to show how these chemical and physical properties can be exploited to target any combination of these regions with pairs of dopants.

As discussed in the introduction, mesostructured sol−gel thin films templated by ionic surfactants possess the three distinct regions depicted in Figure 1. Three strategies for placing molecules preferentially in any one of these regions are

demonstrated here. The first is termed philicity and is summarized by "like dissolves like". Organic compounds are dissolved by the hydrophobic interior of micelles, ionic compounds will accumulate at the ionic interface, and polar molecules may accumulate inside the polar silicate pores. The second strategy is termed bonding. Bonding entails the use of molecules derivatized with trialkoxysilyl groups that can cocondense with the silica precursors in the sol to become fully integrated into the silicate framework of the final film. In other cases, the bonding strategy may apply to covalent grafting of functional molecules to surfactants, thereby placing the dopants in the hydrophobic core of the films. The third strategy is termed bifunctionality, and it applies to molecules that simultaneously incorporate both of the above strategies. These molecules possess both a physical affinity for a particular region and the capability to bond to another. An example is the singly silylated $Ru(bpy)_2ATT$, which has the capability to bond to the silicate matrix and an affinity for the ionic region of the films.

Bifunctionality and Philicity. The bifunctional/philicity strategy is shown by placing $Ru(bpy)_2(ATT)^{2+}$, shown in Figure 2, in the silicate region of the film while simultaneously placing the hydrophobic pyrene molecule in the organic region. The resulting mesostructured films had a *d* spacing of 34.0 Å, and the placement of these molecules into their respective regions is confirmed by luminescence.

The ruthenium complex has its emission maximum at 669 nm in both the amorphous and the mesostructured film (Figure 3). Because the emission maximum is the same in both the amorphous and the mesostructured film, it is evidence that the ruthenium complex resides in the same type of environment, the silica region, in both films. In a previous communication, it was shown that this ruthenium complex shows a blue shift in its emission from 665 to 650 nm when the complex is located in the interface region of the film. The surfactant used in that study was the anionic surfactant SDS. The spectroscopic results suggest that the electrostatic repulsion between the positively charged Ru complex and cationic CTAB headgroups makes the ionic region less hospitable than the micropores of the silicate matrix, thus forcing the Ru complex into the silicate matrix.

Because of its hydrophobic nature, pyrene is located primarily in the organic region of the film, within the hydrophobic tails of the CTAB surfactant, but it is possible that there is a distribution of pyrene molecules among the three regions of mesostructured film. The vibronic structure in the emission spectrum is an indicator of the polarity of the pyrene environment. Here, the mesostructured film templated with CTAB has a very well-resolved vibronic structure, but in the amorphous film the vibronic peaks are not well resolved, only a broad peak is observed, and the intensity is one-half of that of the mesostructured film (Figure 3). These results suggest that pyrene resides mainly in the organic region.

The upper limit on Ru doping with $Ru(bpy)_2ATT$ that still allows mesostructured films to be made is reached at Si:Ru = 50:1. At higher doping levels, the Ru complex increases the silicate condensation rate such that gelation frequently occurs before any films can be drawn. Ambient humidity also becomes crucial to film formation in these syntheses. Below a threshold relative humidity, mesostructured films could not be obtained. Previous studies have shown that micelle formation occurs in the water-rich region of the evolving film.[10,38,39] Consequently, incomplete micelle formation coupled to more rapid condensation (by virtue of the dopant) results in amorphous films at high $Ru(bpy)_2ATT$ concentration.

Bonding and Philicity. The Eu-SL complex is covalently linked to the templated silica network by using a silylated ligand to coordinate the Eu^{3+} ions, and the Tb-OL complex ultimately occupies the organic region of the surfactant micelles. As we showed previously,[9] well-ordered films exhibiting a 2-D hexagonal mesostructure can be obtained by copolymerization of TEOS and the hexa-silylated Eu:SL complex. The incorporation of Tb:OL organic complexes in the film does not disrupt the structure. A reduced degree of long-range ordering is, however, caused by the presence of the Tb:OL molecules, as can be seen by the broadening of the first diffraction peak corresponding to the (100) Bragg reflection. Furthermore, the addition of Tb:OL induces an increase in the *d* spacing value (42.1 Å vs 38.4 Å without Tb:OL). Such an increase may result from the incorporation of the hydrophobic terbium complex within the surfactant micelles when they are formed at the early stage of the film pulling process. Coordination of Eu^{3+}/Tb^{3+} ions by the SL/OL ligands in the CTAB-templated films is clearly established by the excitation spectra which prove the existence of intramolecular energy transfer from the ligands to the rare-earth ions.

The monoexponential decays recorded in all cases for europium and terbium are indicative of a single average site distribution for each ion. In the case of Eu:SL complex molecules, the presence of multiple $Si(OEt)_3$ functional groups results in the chemical bonding of the luminescent centers within the silica framework. The emission properties of europium in the mesostructured films give us more evidence of the location of this ion in the hexagonal mesophase (Figure 4). The similarities in the emission spectra and in the lifetime values observed for the amorphous and mesostructured films indicate that the Eu^{3+} ions lie in a similar environment in the two types of films. Their emission characteristics are in the two cases typical of organic complexes covalently anchored to a sol−gel silica matrix. For terbium, the relatively longer lifetimes and the higher emission intensities observed in the templated films may be a result of a more hydrophobic environment as compared to a pure silica network. The red-shift of the excitation band can also be ascribed to a modification in the polarity of the Tb:OL surroundings. The hydrophobic character of the fluorescent Tb:OL organic complexes probably leads to specific interactions with the surfactant molecules that direct them to the organic region. Once again, the monoexponential decay profile demonstrates that all Tb:OL molecules reside within the micelles.

In these experiments, 2-D hexagonally ordered films could be obtained at Eu:SL/TEOS ratios up to 1/9 (1/4 when the SL ligand is used alone and is not coordinated to rare-earth ions). This upper limit on the achievable organosilica precursor to TEOS ratio depends on the steric hindrance of the organic functionality and on the ability of the $RSi(OEt)_3$ groups to cocondense to give sufficiently rigid organic/inorganic networks.

(38) Grosso, D.; Babonneau, F.; Albouy, P.; Amenitsch, H.; Balkenende, A.; Brunet-Bruneau, A.; Rivory, J. *Chem. Mater.* **2002**, *14*, 931−939.
(39) Grosso, D.; Babonneau, F.; Albouy, P.; Soler-Illia, G.; Amenitsch, H. *Chem. Commun.* **2002**, 748−749.

Without a rigid silica network about the surfactant micelles, the mesostructure is not retained.

Similarly, the loading of metal complexes or organic molecules that are incorporated in films by hydrophobicity alone is limited because an excess of such hydrophobic molecules will prevent the formation of micelles and their organization into hexagonal arrays. The maximum amount of Tb:OL complexes that can be introduced without disrupting the 2-D hexagonal structure of the films corresponds to a Tb:Si molar ratio of about 1:60.

Bonding and Philicity. In another example of this combination of strategies, the silanized $Ru(bpy)_3(PF_6)_2$ was used to ensure its incorporation in the silicate regions, and naphthoquinone was guided to the hydrophobic core of the micelles by virtue of its hydrophobicity. The film structure was characterized by XRD, and the luminescence of the ruthenium complex, which is sensitive to the environment of the molecule, confirmed its location in the silicate matrix of the films.

A small amount (Ru:Si $\approx$ 1:225) of the silanized ruthenium complex was used in these experiments. Films show the typical hexagonal mesostructure at CTAB concentrations higher than 3.5 wt %, with a more highly ordered structure at 4 wt %. The incorporation of NQ did not disrupt micelle formation, and the long-range order structure remained.

A red-shift in the emission maximum of the phosphorescent triplet state of the metal−ligand charge-transfer (MLCT) band of $Ru(bpy)_3^{2+}$ is an indication of a nonpolar environment.[40,41] In this case, the luminescence spectra showed a negligible shift between templated films and amorphous films. Therefore, the silanized ruthenium complex is most likely situated in the silicate framework. In addition, the silica film prepared from a mixture of the silicate sol and NQ did not show any characteristic luminescence of NQ. This indicates that NQ could not be incorporated into the films without the presence of hydrophobic micellar cores.

A luminescence lifetime measurement was carried out to determine if electron-transfer quenching occurred between the electron donor and acceptor in the mesostructured film. The redox properties of these molecules are appropriate for photoinduced electron transfer. Within experimental error, the lifetimes and distribution of the lifetime components were the same among all of the samples (Table 2). Hence, electron transfer was not observed, and its absence suggests that the molecules are too far apart.[33] To prove that the separation between the donor and the acceptor was not the result of low concentration, samples with a higher concentration of either the electron donor or the acceptor were studied. The absence of electron transfer in these films as measured by luminescence lifetimes strongly supports the spatial separation of donor and acceptor in different regions of the films.

Bonding and Bifunctionality. In this experiment, the bonding strategy was employed toward the goal of placing one molecule, the Eu-S4 complex, in the silicate framework of the films and placing another, the singly silylated $Ru(bpy)_2$ATT, in the organic region. XRD verified that structured films containing both lumophores were successfully produced, and luminescence spectra verified the presence of both components in the films.

The XRD diffraction peaks at 2.80° and 5.50° obtained from films containing CTAB are indicative of a hexagonal, close-packed array of cylindrical CTAB micelles. Hence, these films are mesostructured, and films lacking CTAB are amorphous.

The fluorescence spectra from both films show the characteristic emission of each metal complex. The $Ru(bpy)_2$ATT complex has a broad molecular emission between 600 and 700 nm and peaks at approximately 670 nm. Protruding from this envelope are the sharp lines of Eu^{3+} at 592, 616, and 694 nm (Figure 6). The $Ru(bpy)_2$ATT fluorescence maximum is observed near 670 nm in these films, identical to that observed in the Ru−Py films which were also templated with the cationic surfactant CTAB, but different from the maximum observed in films templated by SDS, an anionic surfactant. This discrepancy cannot be attributed to the Eu^{3+} emission line at 694 nm because it is sharp and weak. This similarity of the results to those obtained from the Ru−Py system suggests that the Ru complex resides in the silicate matrix because the cationic surfactant repels the positively charged complex.

Philicity. In these experiments, the affinity of two laser dyes, C540A and R6G, for the organic core of micelles was exploited to place them in that region simultaneously. The structure of the resulting films was verified by the XRD patterns consistent with a 2-D hexagonal packing of cylindrical CTAB micelles with a resulting lattice spacing of 37.1 Å based on a (100) 2θ value of 2.40°.

Excitation and emission spectra demonstrated where the dye molecules were located. Figure 7 shows the emission spectra for films containing the individual laser dyes and the spectrum for the film containing both. The evidence for the localization of the laser dyes comes from the solvatochromic shift of R6G spectra and the intensity difference between emission from amorphous films and emission from mesostructured films for both dyes. The excitation and emission maxima of R6G in amorphous films are identical to the absorption and emission maxima, respectively, of R6G in ethanol solution. Because the excitation and emission maxima of R6G in mesostructured films are red shifted relative to the corresponding maxima in amorphous films (and in ethanol solution), the R6G's environment in mesostructured films is different from that in amorphous films. Because the major difference between the films is the presence of CTAB micelles, it is concluded that R6G resides within the micelles. Such solvatochromism is typical of laser dyes[42] and other chromophores.[43]

The order of magnitude increase in intensity obtained from mesostructured films relative to amorphous films provides further evidence that both laser dyes reside in the surfactant micelles. Self-quenching and aggregate formation are well-known phenomena in organic fluorophores at high concentrations.[44−46] (R6G is dispersed in Triton X100 micelles to increase quantum yield in some laser applications.[47]) The R6G concentrations used here are orders of magnitude smaller than those

(40) Kunjappu, J. T.; Somasundaran, P.; Turro, N. J. *J. Phys. Chem.* **1990**, *94*, 8464.
(41) Meisel, D.; Matheson, M. S.; Rabani, J. *J. Am. Chem. Soc.* **1978**, *100*, 117.
(42) Renge, I. *J. Phys. Chem. A* **2000**, *104*, 7452−7463.
(43) Arabei, S.; Pavich, T.; Galaup, J.; Jardon, P. *Acc. Chem. Res.* **1999**, *32*, 303−313.
(44) Badley, R. Fluorescent probing of dynamic and molecular organization of biological membranes. In *Modern Fluorescence Spectroscopy*; Wehry, E., Ed.; Plenum Press: New York, 1976; Vol. 2, pp 113−119.
(45) Toptygin, D.; Packard, B.; Brand, L. *Chem. Phys. Lett.* **1997**, *277*, 430−435.
(46) Wirnsberger, G.; Yang, P.; Hurang, H.; Scott, B.; Deng, T.; Whitesides, G.; Chmelka, B.; Stucky, G. *J. Phys. Chem. B* **2001**, *105*, 6307−6313.
(47) Valdes-Aguilera, O.; Neckers, D. *Acc. Chem. Res.* **1989**, *22*, 171−177.

that produce fluorescent aggregates in films.[48] Hence, the intensity difference is most likely due to quenching by proximal dye molecules and nonfluorescent aggregates, interactions that become negligible once the dye molecules are subsequently dispersed in CTAB micelles. Such enhancement of fluorescence by surfactants is consistent with previously reported accounts of R6G,[46,48,49] C540A,[50] and other dyes[43,51,52] in similar matrixes.

Although C540A does not exhibit as strong a solvatochromism as R6G, it does exhibit an increase by a factor of 10 in fluorescence intensity on going from amorphous films to mesostructured films. This enhancement of fluorescence by CTAB suggests that C540A suffers from the same self-quenching mechanism that R6G exhibits in amorphous films. Hence, it is reasonable to conclude that C540A resides in either the organic or the interfacial region because self-quenching is suppressed when C540 molecules are dispersed in CTAB micelles. However, because of its hydrophobicity, it is more likely that C540A is partitioned predominantly in the organic region.

Thus far, the concentrations of polar or ionic laser dyes used in these syntheses have not posed any obstacles to structured film formation primarily because their efficient fluorescence allows for obtaining results with fairly small concentrations and because they are highly soluble in our sol system: adding as much as 0.5 g of R6G to the sol still yields homogeneous films with long-range order. The use of hydrophobic dyes, however, is limited because, like NQ, they are slightly soluble in sols with surfactant and insoluble in sols without surfactant.[53]

Summary

Two different luminescent molecules are placed in two different spatially separated regions of mesostructured thin films in a one-step, one-pot preparation using the strategies of philicity (like dissolves like), bonding, and bifunctionality. The strategies take advantage of the different chemical and physical properties of the inorganic silicate framework, the hydrophobic organic interior, and the ionic interface between them. Luminescent molecules that possess the physical and chemical properties appropriate for the desired strategies are chosen. In all cases, the long-range order templated into the thin film is verified by X-ray diffraction. The locations of the molecules are determined by luminescence spectroscopy and by luminescence lifetime measurements. The sensitivity of these techniques enables measurements to be made on films less than 2000 Å thick.

The bonding strategy uses molecules derivatized on all sides by $-Si(OR)_3$ functional groups that condense with other molecules including TEOS to form the framework. The philicity strategy demonstrated in this study takes advantage of hydrophobic molecules that are preferentially localized in the hydrophobic organic interior of the micelles. The bifunctional strategy is a simultaneous combination of both of the above strategies except that only one side of the molecule contains the $-Si(OR)_3$ functional group. When the opposite side of the molecule is the $-Ru(bpy)_2^{2+}$ luminophore, a surprising result is obtained: the luminophore is incorporated in the ionic region when a negatively charged surfactant is used as the templating agent, but it is repelled into the silicate framework when a positively charged surfactant is used.

The simultaneous placement of two molecules in the structured film and the maintenance of long-range order require a delicate balance among film preparation methodology, design of the molecules to be incorporated in specific regions, and concentrations of all of the species. This balance imposes limits and poses challenges for preparation of films with long-range order. It is necessary to maintain the balance among the processes that occur simultaneously during mesostructured film formation including solvent evaporation, micelle formation, and silica condensation that permanently cements the mesostructure in place. In principle, many molecules may be placed as long as this balance is maintained. The successful development of strategies and methods to fulfill these conditions and the proof that active molecules are placed in chosen regions open the possibility of multiple applications of these functional films based on energy transfer, electron transfer, and charge separation.

Acknowledgment. This work was made possible by grants from the National Science Foundation (DMR 0103952 and CHE 0102623). A.-C. Franville thanks the NATO scientific committee for its "Chercheurs Confirmès" research grant. We would also like to thank Prof. H. Monbouquette for the use of his fluorolog spectrometer. P. Minoofar acknowledges Amy Durisin for valuable assistance in the synthesis of films.

JA020817N

(48) Hungerford, G.; Suhling, K.; Fereira, J. *J. Photochem. Photobiol., A* **1999**, *129*, 71−80.
(49) Baker, G.; Jordan, J.; Bright, F. *J. Sol.-Gel Sci. Technol.* **1998**, *11*, 43−54.
(50) Gu, G.; Ong, P.; Li, Q. *J. Phys. D: Appl. Phys.* **1999**, *32*, 2287−2289.
(51) Pal, S.; Sukul, D.; Mandal, D.; Sen, S.; Bhattacharyya, K. *J. Phys. Chem. B* **2000**, *104*, 2613−2616.
(52) Sarkar, A.; Chakravorti, S. *J. Lumin.* **1998**, *78*, 205−211.
(53) Minoofar, P.; Hernandez, R.; Franville, A.; Dunn, B.; Zink, J. *J. Sol.-Gel Sci. Technol.* **2002**, in press.